Synthesis of Poly(methyl methacrylate) Nanoparticles Initiated by Azobisisobutyronitrile Using a Differential Microemulsion Polymerization Technique

Chaiwat Norakankorn,[1] Qinmin Pan,[2] Garry L. Rempel,[2] Suda Kiatkamjornwong[3]

[1]*Faculty of Science, Department of Materials Science, Chulalongkorn University, Bangkok, Thailand*
[2]*Faculty of Engineering, Department of Chemical Engineering, University of Waterloo, Ontario, Canada*
[3]*Faculty of Science, Department of Imaging and Printing Technology, Chulalongkorn University, Bangkok, Thailand*

Received 29 January 2008; accepted 14 December 2008
DOI 10.1002/app.29911
Published online 19 March 2009 in Wiley InterScience (www.interscience.wiley.com).

ABSTRACT: Nanosized poly(methyl methacrylate) (PMMA) particles with a high molecular weight of 10^6 g mol^{-1} and a polydispersity index of about 1–2 were synthesized, for which 2,2′-azobisisobutyronitrile was used as the initiator and a differential microemulsion polymerization technique was employed. The kinetics of the polymerization, the glass transition temperature, tacticity, the particle size distribution, and the morphology of the nanosized PMMA synthesized were investigated. The dependence of the number of the polymer particles (N_p) and the number of the micelles (N_m) on the concentration of the surfactant was discussed. The molecular weight distribution was found to be nearly constant over the polymerization time, which was attributed to the significance of micellar polymerization. The resultant nanosized PMMA has a rich syndiotactic configuration (53–57% rr triads) with a glass transition temperature of about 125°C. A beneficial operation condition was discovered where the conversion reached a maximum at a high monomer-to-water ratio.

Key words: nanoparticles; poly(methyl methacrylate); differential microemulsion polymerization; glass transition temperature; tacticity; morphology

INTRODUCTION

Synthesis of nanosized polymer particles continues to receive increasing attention because of their important potential utilization in various fields, such as drug delivery,[1] protein separation,[2] environmental application,[3] and semiconductors.[4] The most common approach used to synthesize polymer nanoparticles is via microemulsion polymerization.[5–13] However, the major concern with this approach is that it usually requires a high amount of surfactant and it is difficult to decrease the particle size. Surfactants are not only expensive but also have a significantly negative impact on the properties of the synthesized polymers.

To explore a practical technical route in which the surfactant amount required could be significantly decreased and by which the nanoparticle size could be controlled, a differential microemulsion polymerization was proposed,[14] in which the monomer was added in very small drops and the time interval between each drop addition was very short. It was found that the amount of the surfactant required was indeed much lower when compared with other methods reported in the literature.[14–16] It was confirmed that, by using the differential microemulsion polymerization method, the reaction conditions could be milder for regular emulsion polymerization processes, whereas the particle size realized was similar to or even smaller than that produced by microemulsion polymerization. When a differential microemulsion polymerization system is used, particles with a size of less than 20 nm could be controllably synthesized via either a homogeneous nucleation mechanism[14,15] or a heterogeneous nucleation mechanism.[16] It has been found that by using an oil-soluble initiator,[16] smaller poly(methyl methacrylate) (PMMA) nanoparticles were produced and a smaller amount of surfactant is required in the differential microemulsion polymerization than when using a water-soluble initiator.[14,15]

As a continuation to our previous short communication, where we reported on the preliminary success of using the differential microemulsion

Correspondence to: G. L. Rempel (grempel@cape.uwaterloo.ca) or S. Kiatkamjornwong (ksuda@chula.ac.th).
Contract grant sponsor: Thailand Research Fund (TRF); contract grant number: PHD/0269/2545.
Contract grant sponsors: Natural Sciences and Engineering Research Council of Canada (NSERC), Canada Foundation for Innovation (CFI).

polymerization method to achieve the synthesis of PMMA nanoparticles of less than 20 nm,[16] this article reports on a further investigation on the synthesis of PMMA nanoparticles via differential microemulsion polymerization using an oil-soluble initiator, by extending the investigation into the particle population and micelle population in the reaction system, and the tacticity and the glass transition temperature of the resultant polymer in addition to the detailed investigation with respect to the effects of polymerization time, concentration of surfactant, and monomer/water weight ratio on the particle size, molecular weights, and their distribution. Furthermore, the nucleation mechanism was also discussed.

EXPERIMENTAL DETAILS

Materials

Methyl methacrylate (MMA) containing 10 ppm of an inhibitor (AR grade from Aldrich, Milwaukee, WI), sodium dodecyl sulfate (SDS) powder (97% purity from Aldrich), 2,2′-azobisisobutyronitrile (AIBN) (AR grade from Polysciences, Warrington, PA), hydroquinone (HQ; AR grade from Polysciences, USA), methanol (practical grade), and cyclohexane (AR grade from Aldrich) were used as received. Deionized (DI) water was used as obtained from the Department of Chemical Engineering at the University of Waterloo, Ontario, Canada.

Preparation of PMMA microemulsions

Nanoparticles of PMMA were prepared by differential microemulsion polymerization using an oil-soluble initiator AIBN as mentioned in our previous work.[16] The polymerization recipes are given in Table I. The initiator and surfactant were mixed in a specified amount of water in a 500-cm^3 Pyrex glass reactor (Aldrich, Oakville, Ontario, Canada), which was equipped with a double-jacket condenser and a dropping funnel for the addition of the monomer feed. The system was subsequently subjected to heating up to 70°C under constant agitation (200 rpm) provided by a magnetic stirrer bar using a stirring/temperature controlled digital hotplate system (Cole Parmer, Montreal, Quebec, Canada) with a constant nitrogen feed to the reaction vessel through a gas inlet tube. The monomer was fed very slowly under continuous dropping of monomer droplets for a designated time (around 1.5 h) after the temperature of the system had reached 70°C. After the monomer feeding was completed, the reaction system was kept at 70°C with constant agitation for another hour (aging time) to obtain a higher conversion of the polymer.

To quench the reaction, the polymerization system was cooled down by placing the reactor in a bath of cold water at about 10°C for 10 min. Then, the product at ambient temperature was mixed with 5 cm^3 of a 3% solution of HQ in DI water to fully terminate the reaction.

TABLE I
Polymerization Recipes

Water (cm^3)	MMA (cm^3)	AIBN (g)	SDS (g dm^{-3})
60	14	0.08	1.4–23.3
84	14	0.08	1.0–16.7

Compared with the experiments done by He et al.,[14] a cosurfactant, 1-pentanol was not used in this work, and AIBN was used rather than ammonium persulfate (APS) as the initiator.

Separation of polymer samples for characterization

The resultant polymer was precipitated using an excess amount of methanol and it was separated by a vacuum-filtration technique, and the surfactant and initiator were washed with a sufficient amount of warm DI water and methanol. The unreacted monomer was removed by extraction using cyclohexane at 37–40°C for 24 h.

Measurement and calculation of the polymerization conversion

To avoid the effect of periodic sampling on the reaction system during the reaction, sampling was done only at the end of the reaction, i.e., no sampling was done before the reaction was terminated. Thus, for each single reaction operation with a reaction time t, one conversion X_m was obtained. The polymerization conversion (X_m) was obtained by gravimetric analysis and is defined as follows:

$$X_m = \frac{(\text{wt \% of cleaned PMMA particles})_t}{(\text{wt \% of MMA feed})_t} \times 100\% \quad (1)$$

Concentrations of latex particles (N_p) and micelles (N_m)

The concentrations of latex particles (N_p) and micelles (N_m) are calculated according to the following equations:

$$N_p = \frac{6M_0X_n}{\pi\rho(D_n)^3} \quad (2)$$

$$N_m = \frac{([S] - \text{CMC})}{m} \quad (3)$$

where M_0 is the initial concentration of monomer (g dm^{-1}), X_n is the weight ratio of the polymerization conversion, ρ is the density of PMMA (1.18 g cm^{-3}

TABLE II
Dependence of Tacticity of PMMA Latex Nanoparticles on the Concentrations of SDS, Water, and Monomer at the Reaction Time = 2.5 h

Water/ MMA	[SDS] (m*M*)	D_n (nm)[16]	$M_w \times 10^{-6}$ [16]	$M_n \times 10^{-6}$ [16]	% Tacticity			T_g (°C)
					rr	mr	mm	
60/14	4.91	48	2.28	1.17	56	38	6	123
60/14	5.78	24	3.75	1.86	57	37	6	120
60/14	17.34	22	2.69	1.57	54	39	7	119
60/14	40.45	16	1.02	6.95	55	38	6	124
60/14	80.91	16	1.15	7.64	56	37	7	123
84/14	3.51	83	2.41	1.37	55	39	7	122
84/14	4.13	30	3.02	1.80	54	39	8	122
84/14	12.38	20	2.73	1.62	53	39	7	121
84/14	28.89	18	1.19	7.43	56	38	7	124
84/14	57.79	17	1.12	0.73	53	39	8	125

rr = syndiotacticity; mr = atacticity; mm = isotacticity.

at 25°C), D_n is the particle size (nm; Table II), [S] is the concentration of surfactant (m*M*), CMC is the critical micelle concentration of SDS (m*M*), and "*m*" is the number of SDS molecules present in a micelle (i.e., an aggregation number). The value of *m* is 71 based on spherical micelle formation,[17] and the CMC is 8.2 m*M* at 25°C[17] as determined via an electrical conductivity measurement.

Molecular weight average and its polydispersity index

The average-molecular weight ($\overline{M}_n$ and $\overline{M}_w$) and polydispersity index (PDI, equivalent with $\overline{M}_w/\overline{M}_n$) were determined by gel permeation chromatography using a multi-angle laser light scattering setup (GPC-MALLS, Wyatt Technology Corporation, Santa Clara, CA) equipped with a RI detector (Water 150-CV refractive index detector, Waters Limited, Mississuaga, Ontario, Canada) and MALLS detector (DAWN®DSP-F laser Photomer, Wyatt Technologies) in THF at 25°C. A PL-Gel® column setup (Polymer Laboratories, Amherst, MA) was employed consisting of three 300 mm × 8 mm columns.

Measurement of polymer particle size and its distribution

The number-average particle size (D_n) and the distribution of the particle size were measured using a dynamic light scattering technique[16] (DLS, Nanotrac Instrument, Largo, FL).

Tacticity measurement

A Bruker Biospin DPX-300 NMR spectroscometer (Bruker AXS Inc., Madison, WI) was used for ^{1}H-NMR analyses at 300 MHz with $CDCl_3$ solutions at room temperature. The tacticities of the samples were characterized from the integrated ratios of the syndiotactic (rr), isotactic (mm), and heterotactic (mr) triad signals of α-methyl protons, which occur at 0.81, 0.99, and 1.18 ppm, respectively.[11,12]

Glass transition temperature (T_g)

The T_g values of the polymer were measured using a NETZSCH (NetzschInstrument Inc., Burlington, MA) DSC-204 F1 differential scanning calorimeter; a 10-mg sample was used at a scanning rate of 10°C min^{-1} from 25 to 180°C followed by a rapid cooling and heating again at the same rate of 10°C min^{-1}. Mercury (mp = −38.8°C), bi-benzene compound (mp = 69.2°C), indium (mp = 156.6°C), tin (mp = 231.9°C), and bismuth (mp = 271.4°C) were used to calibrate the instrument. The T_g values from the second heating operation were recorded to ensure that the system had reached its thermal steady state during T_g analysis. The T_g was determined using a midpoint method.

RESULTS AND DISCUSSION

Dependence of polymer particle population on concentration of surfactant

The relationships between the concentrations of polymer particles/micelles and surfactant are presented in Figure 1. The concentration of polymer particles (N_p) and micelles (N_m) increased with the increase in the concentration of the surfactant; however, the ratio of N_p/N_m decreased with the concentration of the surfactant. Figure 1 demonstrates that over the experimental range investigated, the concentration of polymer particles increased from 2.04 to 147 μ*M* when the ratio of the water/monomer was 60/14 (v/v) and from 0.36 to 80.6 μ*M* when the ratio of the water/monomer was 84/14 (v/v). The concentration of micelles increased from 129 to 1024 μ*M* and from 58.9 to 698 μ*M* when the ratios of water/monomer were 60/14 (v/v) and 84/14 (v/v), respectively, at a SDS concentration above its CMC.

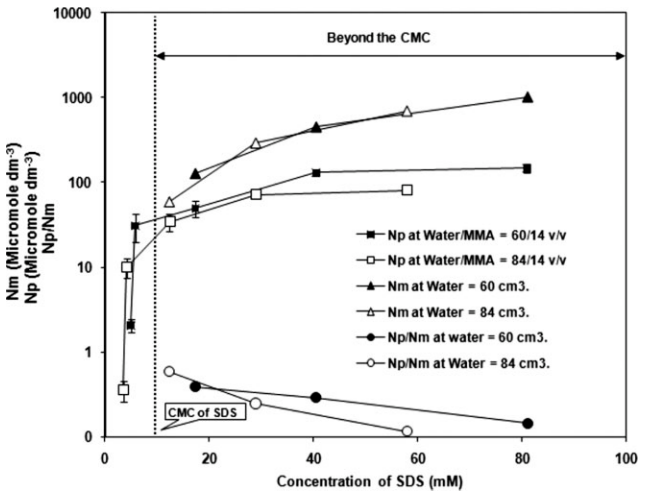

Figure 1 Dependence of N_p, N_m, and their fractions on the concentrations of the surfactants.

The fraction of N_p/N_m decreased from 0.38 to 0.14 and from 0.58 to 0.12 when the ratio of water/monomer was 60/14 (v/v) and 84/14 (v/v), respectively. This phenomenon may be explained by the nature of the nucleation mechanism. Compared with APS, an initiator used in He et al.'s[14,15] work, AIBN used in this work is rather oil soluble, and thus it is believed that a heterogeneous nucleation mechanism[18–21] prevailed in the reaction system employed in this work rather than the homogeneous nucleation mechanism which was proposed in He et al.'s[15] work. The solubility of AIBN is 4×10^{-5} g g^{-1} in H_2O[22] and the partitioning of AIBN between the monomer phase and the water phase is 115/1.[23] Under the assumption that f (initiator efficiency) is equal to 1, the generation rates of AIBN radicals [$(CH_3)_2(CN)C^*$] in the monomer phase and in the aqueous phase at 70°C are 1.61×10^{19} and 1.40×10^{17} dm^{-3} min^{-1}, respectively.[24] The concentration of AIBN radicals generated in the aqueous phase is two orders of magnitude smaller than that in the monomer phase. This suggests that the formation of particle nuclei in the aqueous phase should be rather limited, i.e., heterogeneous nucleation presumably predominates.[24]

Considering the limiting case in which AIBN radicals generated in the micelles predominate in the particle nucleation process, we have found that N_p obtained from the AIBN-initiated polymerization should be less than that obtained from the N_m.[24] So heterogeneous nucleation is observed when the fraction of N_p/N_m was equal or less than 1. The heterogeneous nucleation mechanism is therefore believed to be the predominant particle nucleation mechanism for the high-molecular-weight PMMA nanoparticles as claimed in the previous literature.[16]

Tacticity of PMMA latex nanoparticles

The tacticity of PMMA affects its performance, such as the diffusivity of other materials inside it[12] and its miscibility with other polymers.[25] The ^{1}H-NMR spectrum of PMMA latex nanoparticles is presented in Figure 2. The tacticity of PMMA latex nanoparticles at different concentrations of SDS and different water/monomer ratios is given in Table II. The experimental results show that the tacticity of the PMMA latex nanoparticles at the triad level is almost independent of the concentration of SDS and the water/monomer ratio, which is advantageous for the high syndiotactic PMMA preparation by the differential microemulsion polymerization via the oil-soluble initiator such as AIBN.[16] Possible reasons for the almost independent variation of tacticity with the concentration of SDS and the water/monomer ratio used in the polymerizing mixture were (1) that the primary locus of propagation was in the bulk of the particle and (2) that the tacticity of the chain was not affected by the environment of the particle surface.[12] As with the differential microemulsion polymerization system previously reported, there are no monomer droplets.[15] The reactions in this work are believed to occur within the micelles (heterogeneous nucleation) as the oil-soluble initiator was used. At a higher SDS concentration, there are more micelles that provide more nucleation sites in the system. Furthermore, for the two systems with different MMA/water ratios, at a given SDS concentration, the micelle numbers are believed to be the same after the SDS concentration exceeds the CMC. Thus, according to the different MMA/water ratios in the two systems, each micelle needs to convert a slightly higher monomer amount in the system with a MMA/water = 14/60 v/v than in the system with a MMA/water = 14/84 v/v. Thus, at a given MMA/water ratio or SDS concentration, a higher SDS concentration or MMA/water ratio results in an almost constant percentage of tacticity.

The percentage of syndiotactic PMMA seems to be constant regardless of the SDS concentration as shown in Table III. A random coil of high molecular weight (1×10^6 g mol^{-1}) PMMA has an unperturbed root-mean-square end-to-end distance of 55 nm in the bulk.[12,13] Therefore, a few chains per particle of PMMA made by the differential microemulsion polymerization were toward the low end of the nanoscale (less than 40 nm) leading to the compact size required for more gauche conformations in the polymer chain to reduce its high potential energy in a small particle.[12,13] Therefore, the PMMA formed in a differential microemulsion polymerization is conformationally restricted throughout the reaction.

Nevertheless, the differential microemulsion polymerization of MMA initiated by AIBN produces

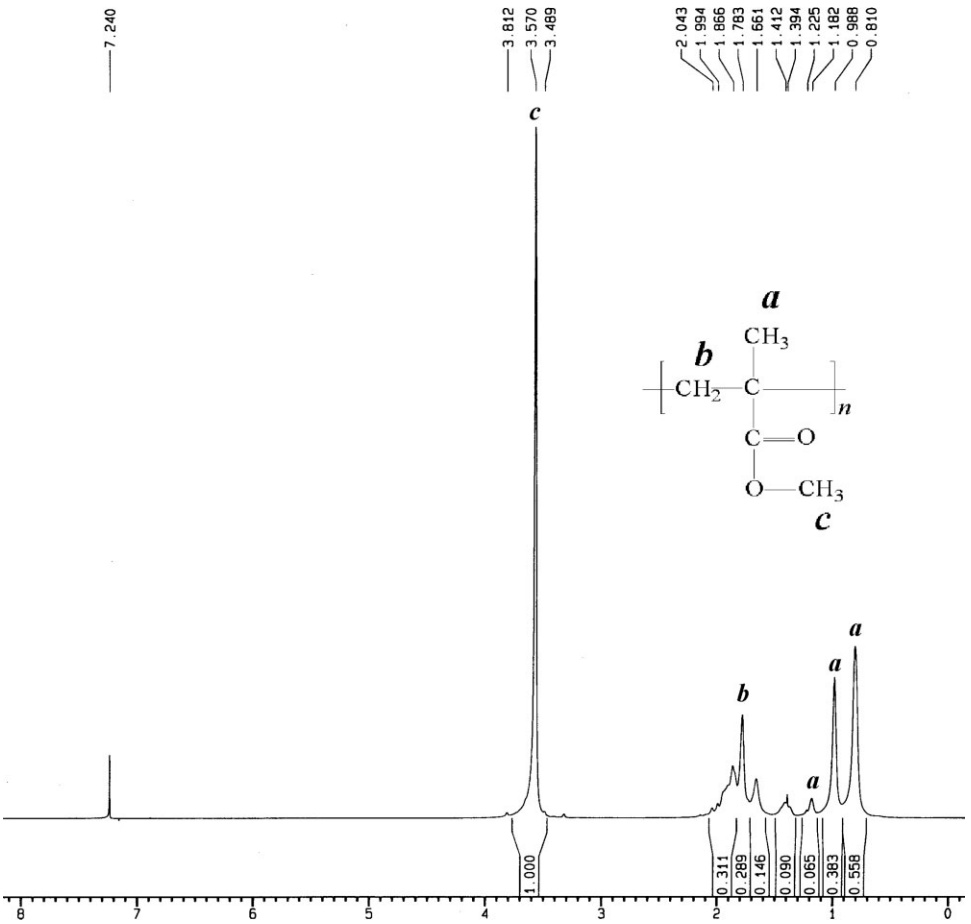

Figure 2 ^{1}H-NMR spectrum of PMMA latex nanoparticles (MMA 14 cm^3, SDS 0.7 g, and water 60 cm^3 polymerized at 70°C for 2.5 h).

predominantly the syndiotactic PMMA containing 53–57% of syndiotactic (rr), 37–38% of heterotactic (mr), and 6–8% of isotactic (mm). The configuration of a PMMA chain in a microemulsion process is more compact than its usual random coil conformation.[12,13] Compared with isotactic PMMA, the syndiotactic PMMA has a lower net repulsive energy and allows the new incoming MMA molecules to easily interact with the growing polymer chains[26] because the syndiotactic configuration of growing polymer chains has two methyl side groups being placed on different planes of the C—C backbone, which provide less steric hindrance. The low potential energy of any configuration of PMMA chains is an important property to stabilize the PMMA chains in the nanoparticle. The syndiotactic PMMA chain

TABLE III
Tacticity and Glass Transition Temperature of PMMA Latex Nanoparticles with Polymerization Times at Water/Monomer Ratio = 60/14

Polymerization times (s)	[SDS] = 5.78 mM				[SDS] = 17.34 mM			
	% rr	% mr	% mm	T_g	% rr	% mr	% mm	T_g
600	–	–	–	–	56	38	6	112
1200	53	39	8	113	56	38	7	110
1800	56	38	6	112	56	38	6	113
2400	56	38	6	117	57	38	5	113
3600	55	39	6	118	57	37	6	111
5400	54	39	7	115	53	39	8	119
7200	56	38	7	114	56	38	6	117

rr = syndiotacticity; mr = atacticity; mm = isotacticity.

exhibits a lower total and intramolecular energy than the isotactic PMMA chain,[26] so the syndiotactic configuration was found much more than the isotactic configuration.

The heterogeneous nucleation of PMMA during synthesis by the differential microemulsion polymerization was a key factor to enhance the rich syndiotactic configuration with the high concentration of PMMA when compared with other microemulsion polymerization techniques.[5–13]

Polymerization conversion (X_m)

The evolution of polymerization conversion (X_m), defined by eq. (1), with respect to polymerization time, is presented in Figure 3. In this study, an oil-soluble initiator AIBN was used, which is sparsely dissolved in water. Because of the special operation procedures in the differential microemulsion polymerization, at the beginning of the polymerization the oil phase may not have a sufficient capacity for the AIBN initiator to be completely dissolved in the system, and thus some AIBN flakes were observed. According to the observation, it was found that a period of 10 min was required to form an oil phase in which all of the AIBN flakes were completely dissolved. The results after 10 min of the reaction time are displayed in Figure 3. According to Figure 3, the X_m–polymerization time curves can be distinguished into three zones: at polymerization times <3600 s (denoted as Zone 1), 3600–5400 s (denoted as Zone 2), and >5400 s (denoted as Zone 3). In Zone 1, the polymerization conversion rapidly increased up to a maximum value of 98.6% for a SDS concentration of 17.3 m*M*, and 67.4% for a SDS concentration of 5.78 m*M* at a polymerization time of 3600 s. In Zone 2, the conversion decreased to 80.7% for a SDS concentration of 17.3 m*M*, and 59.10% for a SDS concentration of 5.78 m*M* at the end of MMA feeding and at a polymerization time of 5400 s. This trend is understandable because there are two factors that affect the polymerization conversion in an opposite manner. During the monomer addition period, on the one hand, with the addition of monomer the denominator in eq. (1) was increased, which decreased the calculated X_m; and on the other hand, at the same time, with the addition of the monomer, the amount of polymer particles was possibly increased; thus the polymerization conversion could be expected to increase. In Zone 1, i.e., at times up to 3600 s, the effect from increasing more polymer particles was possibly dominant, and the polymerization conversion increased with the addition of monomer, as shown in Figure 3. In Zone 2 (the period of 3600–5400 s), the amounts of polymer particles may not increase further or at least the rate of the increase in the amount of polymer particles decreased, which could be caused by a balance between the polymer particle population and micelle population. Thus, most of the further added monomer molecules have to enter into the existing polymer particles, which were larger than the newly nucleated particles, and the time needed for the monomer diffusion into the particles would decrease the polymerization conversion. Thus, the polymerization conversion decreased with the addition of monomer, as reflected in Figure 3. In Zone 3, the addition of monomer had already stopped and thus the denominator in eq. (1) did not increase any more. However, the reaction was still going on; therefore, the polymerization conversion in Zone 3 increased.

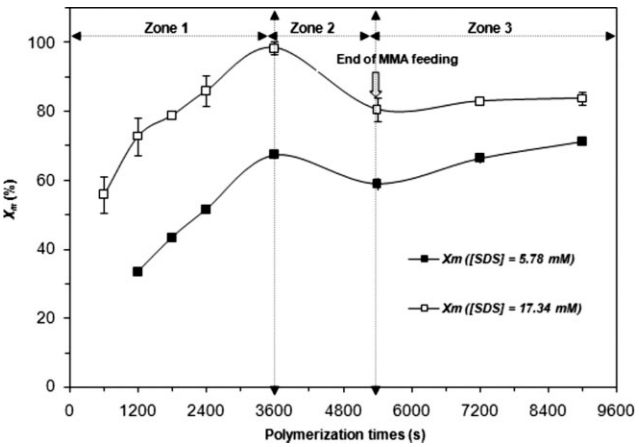

Figure 3 Relationship between the polymerization conversion against the polymerization time of PMMA.

The results of the polymerization conversion indicated that the new particles of PMMA were possibly induced during polymerization more than growth of the existing PMMA particles. In addition, the heterogeneous nucleation was dominated throughout the polymerization time. Then the amounts of syndiotactic configuration were high throughout the polymerization time.

Molecular weight and its PDI

The dependence of the molecular weight and the PDI of the produced polymer over the reaction time at two levels of SDS concentrations (5.78 and 17.34 m*M*) are presented in Figure 4. The molecular weights [$\overline{M}_w$ and $\overline{M}_n$ as shown in Fig. 4(a)] obtained at both levels of SDS concentration did not differ much during the early stages of polymerization up to 7200 s (at which $\overline{M}_w$ changed from about 0.7×10^6 to 1.7×10^6 while $\overline{M}_n$ changed from 4×10^5 to 9×10^5). Unlike the molecular weights, the PDI [shown in Fig. 4(b)] for both levels of SDS concentrations are not much different (at [SDS] = 17.34 m*M*, PDI varied from 1.55 to 1.75, whereas at [SDS] =

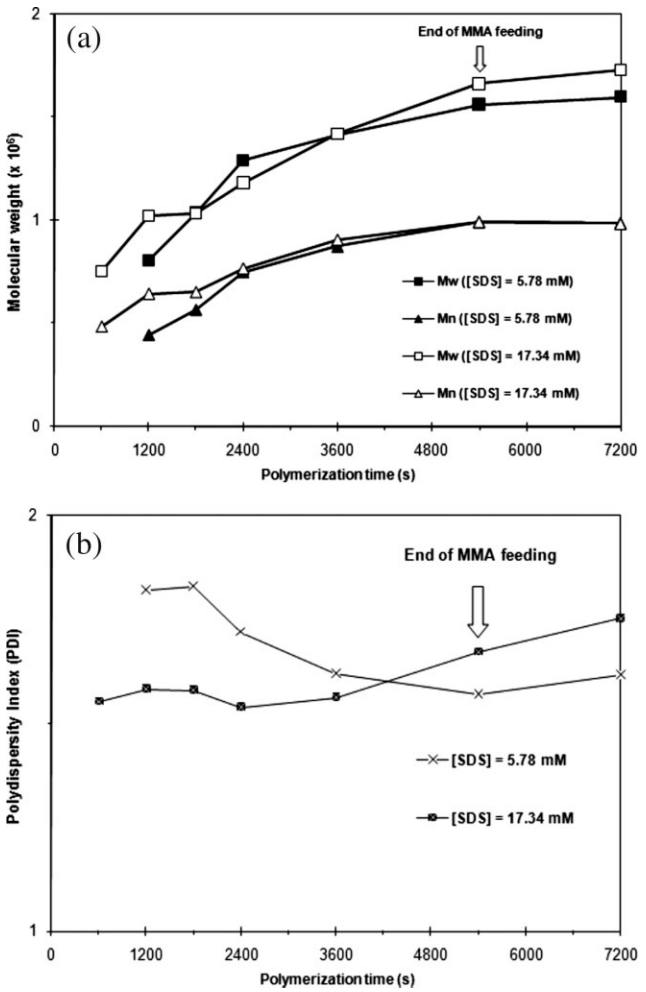

Figure 4 Relationship between the molecular weight and the polymerization time of PMMA microemulsion measured by GPC-MALLS: (a) molecular weight and (b) polydispersity index.

5.78 m*M*, it varied from 1.82 to 1.62). The nearly constant and very narrow value of PDI over the whole range of polymerization time could be attributed to the significance of the restriction of the nanosized reaction sites, which is an advantage of the polymerization method investigated in this work.

T_g of the resultant polymer

According to Table II, the T_g of the synthesized PMMA is almost constant across the whole reaction period. The resultant PMMA nanoparticles synthesized over a reaction time of 2.5 h, as shown in Table III, have a T_g range of 120–125°C, which is significantly higher than the values of 105–107°C generally reported[27] for general polymerization to produce PMMA. The high T_g results from the high molecular weight and the high percentage of syndiotactic configuration[12,13,26] produced by the differential microemulsion polymerization technique. Soldera[26] found that the computed total intramolecular energy for isotactic PMMA is higher than that of syndiotactic PMMA, but syndiotactic PMMA has higher nonbond energy. According to the free volume theory,[28] high interactions between the neighboring polymer chains will give a higher T_g. Therefore, the syndiotactic dominant PMMA has a higher T_g value.

CONCLUSIONS

The differential microemulsion polymerization technique was employed for synthesizing nanosized particles of PMMA having high molecular weight of 10^6 g mol^{-1} using the AIBN oil-soluble initiator. The high-molecular-weight PMMA latex nanoparticles have a rich syndiotactic configuration (53–57% rr triads). The rate of polymerization increased with an increase in the concentration of the SDS surfactant. The nearly constant value of PDI over the whole range of polymerization time could be attributed to the significance of particle nucleation occurring via a heterogeneous nucleation mechanism. The high-molecular-weight PMMA nanoparticles have spherical shape with a T_g of about 125°C. It is very interesting to note that the conversion reaches a maximum within a short reaction time in the presence of less surfactant and without the need of a cosurfactant and with a high monomer-to-water ratio.

References

1. Couvreur, P.; Puisieux, F. Adv Drug Delivery Rev 1993, 10, 141.
2. Salata, O. V. J. Nanobiotechnology 2004, 2, 1.
3. Cumbal, L.; Greenleaf, J.; Leun, D.; SenGupta, A. K. React Funct Polym 2003, 54, 167.
4. Caruso, F. Colloids and Colloidal Assemblies; Wiley-VCH: Weinheim, 2004.
5. Capek, I. Adv Colloid Interface Sci 1999, 80, 85.
6. Capek, I. Adv Colloid Interface Sci 1999, 82, 253.
7. Stoffer, J. O.; Bone, T. J Polym Sci Polym Chem Ed 1980, 18, 2641.
8. Roy, S.; Devi, S. J Appl Polym Sci 1996, 62, 1509.
9. Gan, L. M.; Chew, C. H.; Ng, S. C.; Loh, S. E. Langmuir 1993, 9, 2799.
10. Rodriguez-Guadarrama, L. A.; Mendizabal, E.; Puig, J. E.; Kaler, E. W. J Appl Polym Sci 1993, 48, 775.
11. Gan, L. M.; Lee, K. C.; Chew, C. H.; Tok, E. S.; Ng, S. C. J Polym Sci Part A: Polym Chem 1995, 33, 1161.
12. Pilcher, S. C.; Ford, W. T. Macromolecules 1998, 31, 3454.
13. Jiang, W.; Yang, W.; Zeng, X.; Fu, S. J Polym Sci Part A: Polym Chem 2004, 42, 733.
14. He, G.; Pan, Q.; Rempel, G. L. Macromol Rapid Commun 2003, 24, 585.
15. He, G.; Pan, Q.; Rempel, G. L. Ind Eng Chem Res 2007, 46, 1682.
16. Norakankorn, C.; Pan, Q.; Rempel, G. L.; Kiatkamjornwong, S. Macromol Rapid Commun 2007, 28, 1029.

17. Chen, C.-S.; Lin, C.-H. Polymer 2000, 41, 4473.
18. Gardon, J. L. J Polym Sci Part A-1: Polym Chem 1968, 6, 623.
19. Gardon, J. L. J Polym Sci Part A-1: Polym Chem 1968, 6, 643.
20. Sajjadi, S. Polymer 2003, 44, 223.
21. Hansen, F. K.; Ugelstad, J. J Polym Sci Polym Chem Ed 1979, 17, 3069.
22. Alduncin, J. A.; Forcada, J.; Asua, J. M. Macromolecules 1994, 27, 2256.
23. Nomura, M.; Ikoma, J.; Fujita, K. J Polym Sci Part A: Polym Chem 1993, 31, 2103.
24. Chern, C.-S.; Tang, H.-S. J Appl Polym Sci 2005, 97, 2005.
25. Vorenkamp, E. J.; Brinke, G. T.; Meijer, J. G.; Jager, H.; Challa, G. Polymer 1985, 26, 1725.
26. Soldera, A. Polymer 2002, 43, 4269.
27. Brydson, J. A. Plastics Materials; Butterworth-Heinemann: Oxford, 1999; p 405.
28. Sperling, L. H. Introduction to Physical Polymer Science, 4th ed.; Wiley-Interscience: New Jersey, 2006; p 381.